

---

## Theoretical Studies of MHD Stability

F. Troyon

*Phil. Trans. R. Soc. Lond. A* 1987 **322**, 163-171

doi: 10.1098/rsta.1987.0045

---

### Email alerting service

Receive free email alerts when new articles cite this article - sign up in the box at the top right-hand corner of the article or click [here](#)

---

To subscribe to *Phil. Trans. R. Soc. Lond. A* go to: <http://rsta.royalsocietypublishing.org/subscriptions>

---

## Theoretical studies of MHD stability

BY F. TROYON

*Centre de Recherches en Physique des Plasmas, Association Euratom–Confédération Suisse, Ecole Polytechnique Fédérale de Lausanne, 21 Avenue des Bains CH-1007 Lausanne, Switzerland*

MHD instabilities limit the operating range of a tokamak both in current and pressure. The stability diagram of a low  $\beta$  ohmic plasma is discussed. Examples of instabilities driven by toricity and by pressure are given. Results of optimization lead to a scaling law for the maximum  $\beta$  that can be stably confined. It has not been overcome by experiments so far.

## 1. INTRODUCTION

Since the early days of fusion research rapid loss of confinement through instabilities has been a major concern. The basic time scale  $\tau_A$  of the fastest of these instabilities is given in the case of a tokamak by the Alfvén-wave transit time across the major radius  $R$  of the torus,

$$\tau_A \approx R\sqrt{(\mu_0\rho)}/B,$$

where  $\rho$  is the plasma density and  $B$  the magnetic field. It is always of the order of microseconds or less. In such an instability, the motion is fast compared to the resistive and thermal diffusion time through the plasma so that the magnetic field is frozen and the plasma behaves as an ideal, perfectly conducting fluid. The most violent of these instabilities are destructive and they must be imperatively avoided if the plasma is to exist at all for a substantial amount of time.

Figure 1 shows such an instability, which destroys a straight Z-discharge, which can be viewed as a fraction of a large-aspect-ratio tokamak without any toroidal field ( $B_\phi = 0$ ). The growth time of this short-wavelength, symmetric ( $m = 0$ ) instability would be less than a microsecond for typical plasma parameters in a tokamak. It is easily stabilized by a small amount of toroidal field. Another, slower-growing instability, however, becomes visible. It is called a kink ( $m = 1$ ). The plasma is deformed in a helix, the pitch-length of which increases as the  $B_\phi$  field increases. It is a long-wavelength instability as shown in figure 2 on the same straight discharge. The growth time is only a few times longer than that of the  $m = 0$  mode of figure 1. When the pitch-length of the equilibrium field coincides with the developed tokamak length  $2\pi R$ , which corresponds to the Kruskal–Shafranov condition already given in the introductory lecture of Dr Pease (this symposium),

$$B_\phi = B_{\min} \equiv \mu_0 IR/2\pi a^2, \quad \text{or} \quad I = I_{\text{KS}} \equiv 2\pi a^2 B_\phi / \mu_0 R, \quad (1)$$

the instability changes character, with smaller growth rate and a more complicated internal deformation pattern. When the pitch-length is further increased the plasma becomes grossly stable.

Slower-growing instabilities, which are not always destructive to the confinement, can still manifest themselves. Their consequences are nevertheless important, for example, driving turbulence, which increases transport, inducing changes in the magnetic topology, driving global relaxation phenomena. The instabilities that lead to a redistribution of the magnetic

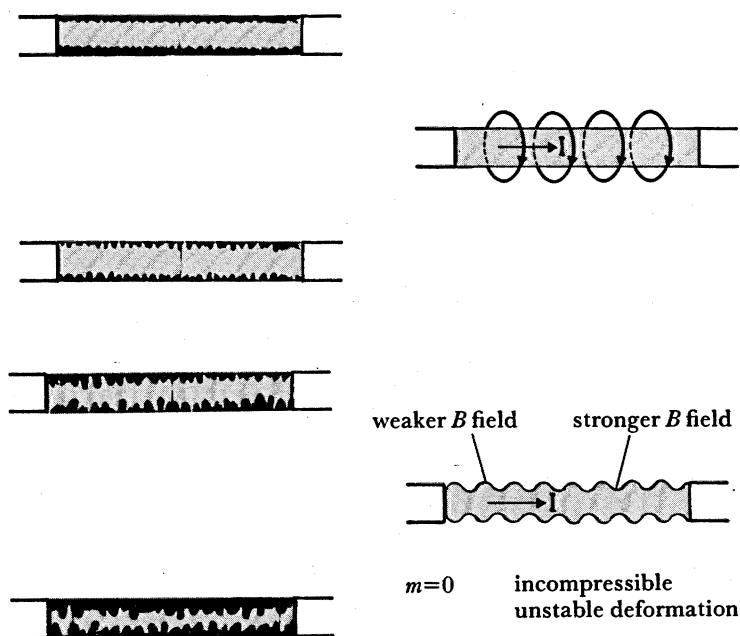


FIGURE 1. Z-pinch ( $B_\theta, B_z = 0$ ). Side views of the evolution of an  $m = 0$  instability in a straight discharge with no axial field. The deformation exponentiates because of the increasing imbalance between the magnetic force and the plasma pressure.

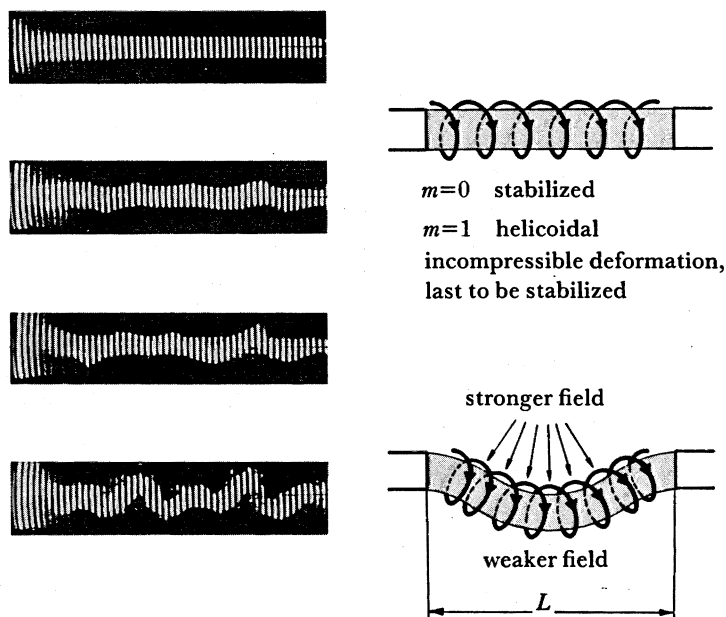


FIGURE 2. Stabilized Z-pinch ( $B_\theta, B_z$  fields). Side views of the evolution of an  $m = 1$  kink instability in the same straight discharge in presence of a small axial field. The deformation is helicoidal and exponentiates at a rate a few times slower than the  $m = 0$  instability of figure 1. The force imbalance due to the higher magnetic force inside the kink drives it away from the straight equilibrium.

flux, although owing to the resistivity, are on a time scale much greater than the global resistive-diffusion time and much less than the duration of a tokamak shot. These so-called resistive instabilities create a braiding of the field lines. The very existence of a tokamak discharge demonstrates that there is an operational range in which there are no fast instabilities and slower-growing instabilities saturate.

This presentation is limited to the description of the fastest ideal MHD instabilities and the operational limits introduced by their onset.

## 2. CURRENT PROFILE AND SAFETY FACTOR

The stability properties depend in an essential manner on a quantity, the safety factor  $q_a$ . In a large-aspect-ratio tokamak with circular cross section it is defined as the ratio of the Kruskal–Shafranov current  $I_{KS}$  to the current passing effectively through the plasma of radius  $a$ ,  $I$ ,

$$q_a = I_{KS}/I = B_\phi 2\pi a^2 / \mu_0 RI \equiv B_\phi a / RB_p, \quad (2)$$

where  $B_p$  is the poloidal field on the plasma surface. It can be rewritten in terms of the average current density in the plasma  $J_a = I/\pi a^2$

$$q_a = 2B_\phi / \mu_0 RJ_a. \quad (3)$$

Inside the plasma, a local safety factor  $q(\rho)$  is defined by replacing into (3) the average current density  $J_a$  by  $J_\rho = I_\rho/\pi\rho^2$ , where  $I_\rho$  is the current flowing inside the radius  $\rho$ :

$$q(\rho) \equiv 2B_\phi / \mu_0 RJ_\rho = 2\pi\rho^2 B_\phi / \mu_0 RI_\rho. \quad (4)$$

This definition is generalized to any shape and aspect ratio by the formula

$$q = \frac{1}{2\pi} \oint \frac{dl B_\phi}{RB_p}, \quad (5)$$

where the line integration is along a closed poloidal field line,  $R$  is the local distance to the major axis. It has a geometric interpretation. It is the number of times a field line has to turn around the major axis for its image projected on a fixed meridian plane to close on itself.

In ohmically heated tokamaks, the current profile is seen to peak spontaneously, which leads to a monotonically increasing  $q$  profile from the axis ( $q_0$ ) to the surface ( $q_a$ ). The value  $q_0$  stabilizes around 1, the exact value being still not known with certainty. Such a  $q$  profile is the signature of the tokamak.

A tokamak equilibrium is characterized by its geometry (major radius  $R$  and the shape of its minor cross section), the toroidal field, the local current density profile  $j_\phi$  or equivalently its  $q$  profile and the plasma pressure profile  $p$ .

## 3. THE ENERGY PRINCIPLE

The potential energy of the system is the sum of the plasma internal energy ( $\gamma =$  adiabatic index) and of the magnetic energy

$$W_p = \int d^3x \left( \frac{p}{\gamma-1} + \frac{B^2}{2\mu_0} \right). \quad (6)$$

A stable equilibrium corresponds to a minimum of the potential energy, with the proper constraint between the variations of the pressure and of the magnetic field. On the ideal time scale the essential constraint is the freezing of the magnetic field in the fluid. The most convenient way to compute the change in potential energy is to introduce the displacement vector field  $\xi(\mathbf{x}, t)$  of the plasma relative to its equilibrium position.

The second variation of the potential energy is (Bateman 1980)

$$\delta W = \frac{1}{2} \int d^3x \left\{ \frac{1}{\mu_0} |\delta \mathbf{B} + \mu_0 (\mathbf{j} \times \mathbf{n}) \xi_n|^2 + \gamma p |\nabla \cdot \xi|^2 - 2 \mathbf{j} \times \mathbf{n} \cdot [(\mathbf{B} \cdot \nabla) \mathbf{n}] \xi_n^2 \right\}, \quad (7)$$

where  $\mathbf{n}$  is a unit vector in the direction of  $\nabla p$ ,  $\mathbf{B}$  is the equilibrium field and  $\mathbf{j}$  the current density (with both poloidal and toroidal components). In vacuum  $\mathbf{j} = p = 0$ , whereas in the plasma the perturbed magnetic field  $\delta \mathbf{B}$  is related to  $\xi$  by

$$\delta \mathbf{B} = \nabla \times (\xi \times \mathbf{B}). \quad (8)$$

The deformation  $\xi$  can be expanded in a Fourier series in the toroidal angle  $\phi$

$$\xi = \sum_{n=0}^{\infty} \xi^{(n)} e^{in\phi}. \quad (9)$$

Because of the axisymmetry of the tokamak the potential energy is just the sum of the potential energies for each  $n$  so that each  $n$  can be considered independently.

Possible  $n = 0$  instabilities are not considered here. When they occur (for elongated cross section), they are cured with a combination of passive and active stabilization as in JET.

Full stability requires that  $\delta W \geq 0$  for any displacement field  $\xi(\mathbf{x})$ . Simple in principle, this stability criterion has turned out to be very difficult to use in toroidal geometry. The difficulty lies in the fact that the plasma can never be better than marginally stable. Straightforward numerical minimization of the potential energy will introduce an error which can be stabilizing or destabilizing and it is then difficult to separate the numerical inaccuracy from an eventual destabilization. Loosely speaking, it is like trying to approximate a flat surface by pieces of curved surfaces. It will never be exactly flat. These difficulties have nevertheless been solved, or at least are well enough understood to be overcome, and there exist now large computer codes (Grimm *et al.* 1976; Gruber *et al.* 1981; Degtyarev *et al.* 1984; Goedbloed *et al.* 1985) suitable to study the stability of any toroidal equilibrium to low- $n$  perturbations. For short wavelengths ( $n \rightarrow \infty$ ) an analytic theory has been developed (Connor *et al.* 1979) which leads to an easy test to be carried out on each isobar, the so-called ballooning mode criterion. There remains a problem with intermediate values of  $n$  and it is generally assumed, but only verified in a couple of cases, that their behaviour is not different from that of the very low  $n$  or very high  $n$ .

#### 4. STABILITY DIAGRAM OF A LOW- $\beta$ OHMIC PLASMA (WESSON 1978; TROYON 1986)

At low  $\beta$ , in a large-aspect-ratio tokamak with circular cross section, stability is conditioned essentially by the two parameters  $q_0$  and  $q_a$ . Figure (3) shows the stable region free of any ideal instabilities even in the absence of any conducting shell around the plasma. It is limited on the left by  $q_0 = 1$ , which is the Kruskal-Shafranov limit applied to the most central plasma

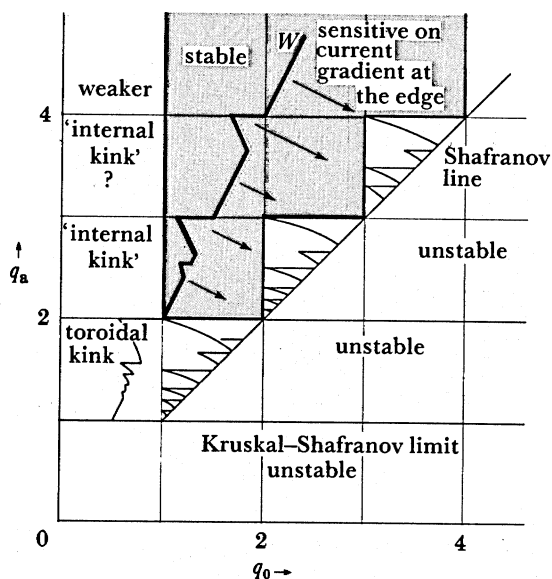


FIGURE 3. The stable operating range of a low  $\beta$ , large aspect ratio circular tokamak in the  $(q_0, q_a)$  plane. The right-hand boundary depends sensitively on the current profile.

region, and by a line  $q_0(q_a)$  on the right, which depends on the current profile. The limit  $W$  is for a current profile

$$j_\phi = j_0(1 - \rho^2/a^2)^\nu, \quad \nu = q_a/q_0 - 1, \quad (10)$$

whereas the line labelled Shafranov corresponds to a current profile

$$j_\phi = \begin{cases} j_0 & \text{for } \rho < \rho_0 \\ 0 & \text{for } \rho_0 < \rho \leq a. \end{cases} \quad (11)$$

The limit is given by the onset of the  $n = 1$  instability but the higher  $n$  limits in the case of the Shafranov profiles are visible to the right of the  $n = 1$  limit. By increasing the current gradient at the plasma edge it is possible to reduce even further the stable region compared with the  $W$  line. The  $W$  line also shows a shrunken stable range in  $q_0$  when  $q_a$  is just below an integer. The Shafranov limit can be considered as the most optimistic case.

Figure 4 shows in a particular meridian plane where the displacement is up-down symmetric, the unstable flow pattern of a  $n = 1$  instability. The interesting feature is that this mode is only unstable because of toroidal curvature. The mode, expanded in a Fourier series in the polar angle  $\theta$  around the magnetic axis is mainly  $m = 1$  inside  $q = 1$  and becomes mainly  $m = 2$  at the surface. This mixing is due to the dependence on  $\theta$  of the various equilibrium quantities. The origin of the instability is due to the  $m = 1$  dependence of the only non-positive definite term of  $\delta W$  (7). The relative phase of the  $m = 1$  and  $m = 2$  components can be chosen such that the interference term is destabilizing. This example illustrates well the two opposite effects of the toroidal geometry: a possible destabilization of the modes due to the interference of the different  $m$  numbers and a stabilization due to the periodicity requirement in  $\phi$ .

We know that the operation diagram of an ohmic low- $\beta$  non-circular tokamak of moderate elongation and D-shaped such as JET still looks qualitatively as in figure 3 but there does not

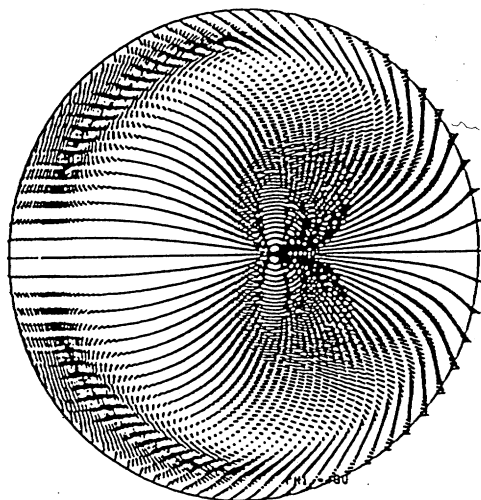


FIGURE 4. Unstable  $n = 1$  free boundary mode in a pressureless circular-cross-section tokamak of aspect ratio 2.5. The current profile is a smoothed rectangular profile (11) with  $q_a = 1.44$ ,  $q_0 = 0.34$ . This configuration would be stable in a straight plasma column. The growth rate is  $0.18 \tau_A^{-1}$ .

seem to have been a real attempt to calculate precisely its boundary. The main point is that the stable domain is limited to the left by a line  $q_0 > 1$  and the domain extends down to about  $q_a \approx 2$ . This appears to remain the limit on the current which can flow in the plasma as long as the shear at the edge (rate of change of  $q$ ) is not too large.

### 5. $\beta$ -LIMITING INSTABILITIES

Increasing the pressure of the plasma reduces the operational space in the  $(q_0, q_a)$  plane, at least for monotonic current profiles of the same class as those considered in the preceding section. The right-hand boundary closes towards the left while the left boundary moves very slowly to the right. Which  $n$  will close in first depends on the pressure profile.

The very-short-wavelength modes ( $n \rightarrow \infty$ ) are sensitive to the local pressure gradient and to the local rate of change of  $q$ , called the shear. For rounded  $q$  profiles with shear varying continuously from the centre to the edge there is a maximum pressure gradient on every surface beyond which the high  $n$  modes are unstable. This leads, when the pressure profile is made marginal everywhere, to a maximum value of  $\beta$ . The local character of the instability is expected to lead to a soft  $\beta$  limit by progressive redistribution of the pressure gradient.

The origin of this instability can be qualitatively understood. The most dangerous deformation of the plasma has an helicity that matches locally that of the magnetic field as well as the periodicity in  $\phi$  allows it. This reduces the perturbed magnetic energy term in (7) to a minimum. Simultaneously by coupling various  $m$ s the amplitude of the mode is maximized in the region where the last term of  $\delta W$  (7) is negative. This is usually on the outside of the torus.

The  $n = 1$  mode is also destabilized by pressure but it appears to feel the total pressure and not much its profile. For example, the  $n = \infty$  limit, which in the absence of a conducting shell close to the plasma always provides a higher  $\beta$  limit than the  $n = 1$  mode, can be brought down much lower than the  $n = 1$  limit by increasing in some region the pressure gradient without shifting the  $n = 1$  limit. Figure 5 shows for, a sequence of JET-shaped equilibria with

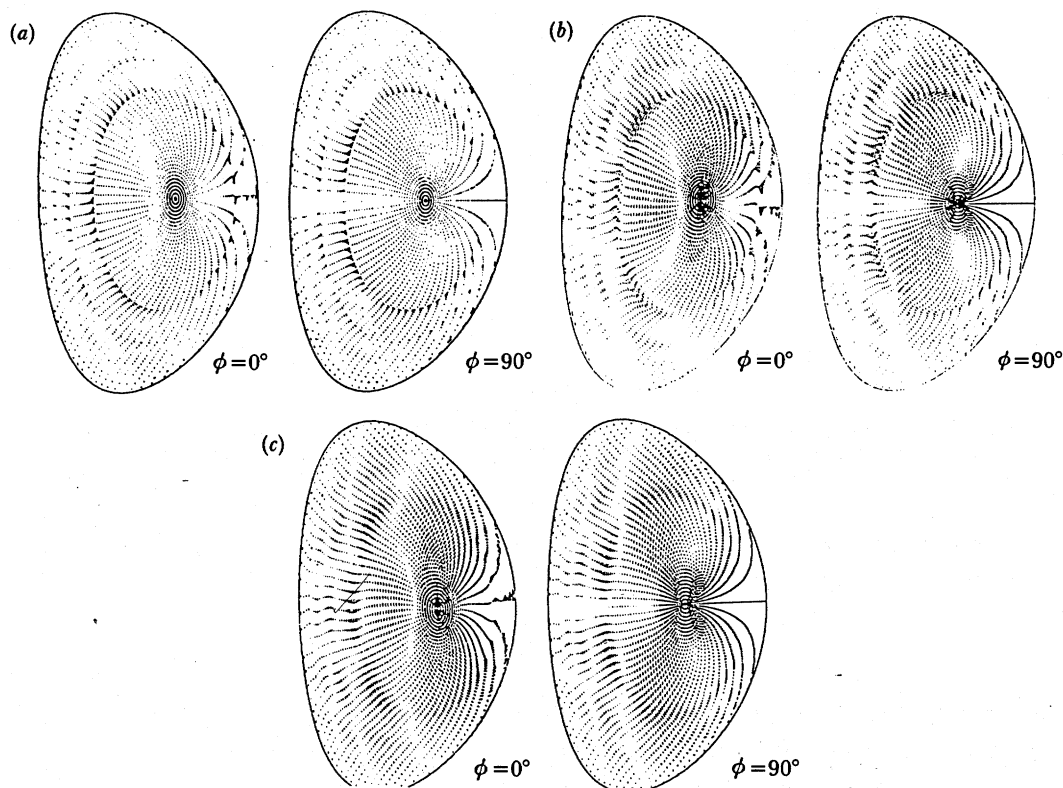


FIGURE 5. (a-c) Maps of the unstable  $m = 1$  poloidal flow pattern in two meridian planes distant of  $90^\circ$  for three JET-shaped equilibria having the same current  $I = 4.8$  MA and almost the same  $q$  profile with  $q_0 \approx 1.15$  and  $\beta$  of 3.2, 3.5 and 4.1 %, respectively. Increasing  $\beta$  increases the growth rate and the mode becomes more global with less internal structure.

current profiles similar to the Wesson profile (Wesson 1978) and increasing  $\beta$ s the map of the unstable poloidal displacement in two meridian planes distant by  $90^\circ$ . Each step in  $\beta$  increases the growth rate by three to four. Peaking of the displacement reveals the location of the singular surfaces. The lowest value of  $\beta$  is close to the marginal point. This instability is expected to be hard because it cannot be suppressed by a local adjustment of the profiles.

Figure 6 shows the result of a series of calculations of the  $n = 1$   $\beta$  limit made with JET parameters ( $B_\phi = 3.45$  T) and the same kind of current profile as described above, with the assumption of always no shell around the plasma (Saurenmann *et al.* 1985). Up to 10 MA which corresponds to  $q_a = 2$  at  $\beta = 0$  there is stability up to a maximum value of  $\beta$ ,  $\beta_{\max}$ . Above this current and up to about 12 MA stability is achieved in a band of  $\beta$ . This is due to the fact that the pressure increases  $q_a$  for a fixed total current  $I$ , so that  $I$  can be further increased without crossing the limit  $q_a \approx 2$ . There has not been an optimization of the dotted line. The striking result is the linear dependence of  $\beta_{\max}$  on the current. The fit corresponds to the formula

$$\beta_{\max} = 2.2I_N \%, \quad \text{where} \quad I_N \equiv \mu_0 I / aB_\phi,$$

where  $a$  is the horizontal half-width of the plasma. The optimum corresponds each time to a current profile such that  $q_0 \approx 1.1-1.2$ .



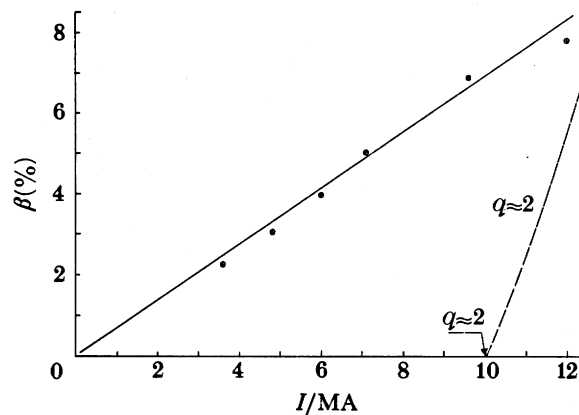


FIGURE 6. The limiting  $\beta$  in JET as a function of the current  $I$ . The circles are results of an optimization  $\beta_{\max}$  stable to  $n = 1$  modes and the line is a fit  $\beta_{\max} = 2.2 I_N$  (%). Along the interrupted line,  $q_a \approx 2$ .

A ballooning optimization carried out with a very similar current profile (Sykes *et al.* 1983) has led to the same scaling law with a higher coefficient

$$\beta_{\max} = 3.2 I_N \%$$

The dependence of  $\beta_{\max}$  on  $I_N$  has been confirmed by optimizations carried out with different aspect ratios and shapes, at least for shapes not too far from circular.

Compilations of existing experimental data (Troyon & Gruber 1985; Overskei & Strait 1986) have shown a surprising agreement with the above scaling law with a coefficient 2.8 between the two values quoted. Newer results obtained on ASDEX have added additional support for the scaling law as well as evidence that the  $\beta$  limit calculated above may only be reached in a transient state, the steady-state value being still lower (von Gierke *et al.* 1985).

## 6. CONSEQUENCES AND PROSPECTS

The scaling law for the  $\beta$  limit only raises a problem when it is coupled with a current limitation. In a tokamak with circular cross section, the maximum current corresponds to  $q_a = 2$ , giving

$$\beta_{\max} = (2.2-3.2) \pi(a/R) \%$$

This value is usually considered much too low for a reactor, more so if the steady-state value has to be reduced further by 30–50% as suggested by the ASDEX and PBX (Princeton machine) results and if one takes into account the helium (ash) and impurities, which reduce the useful pressure.

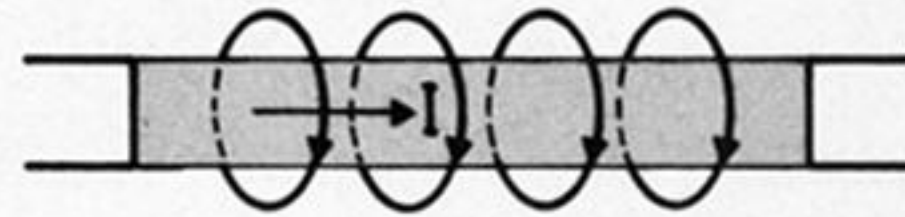
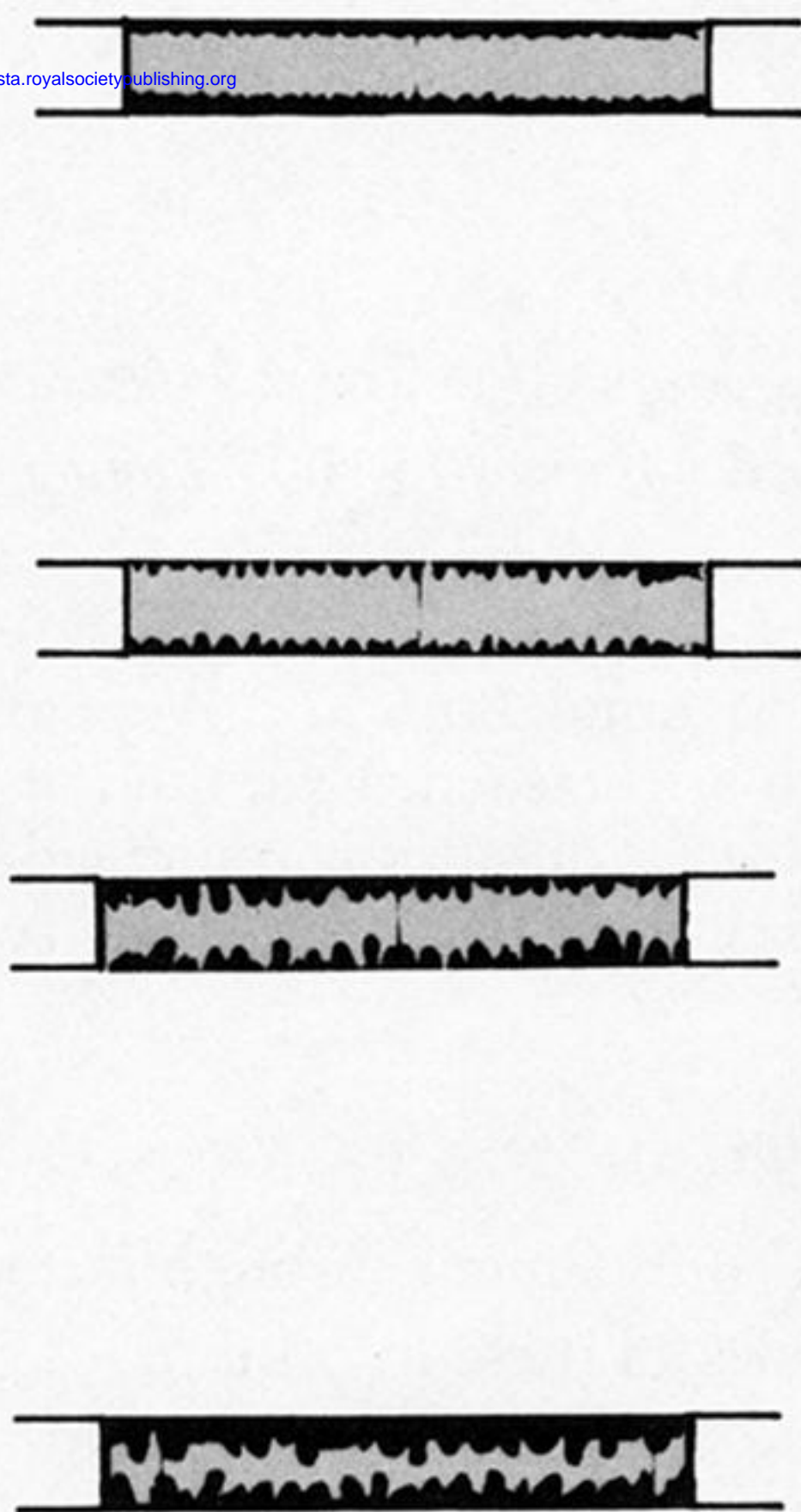
It is thus necessary to improve on this circular limit. In this respect the JET configuration, with the combination of a small aspect ratio and moderate elongation, is remarkable. The maximum current of 12 MA is about 2.5 times the maximum current in a circular plasma and  $\beta_{\max}$  is increased by the same factor. Experimentally, an increase of slightly more than 2 of the current over its circular limit calculated, assuming the radius is equal to the plasma half-width in the equatorial plane, has been achieved in two tokamaks (D-III and PBX) and this is how they have obtained record values of  $\beta$ .

## 7. CONCLUSIONS

Good progress has been made in the understanding of global instabilities in tokamaks and in their influence on the operational limits. Theory has developed to the point where it can start to make specific predictions for any machine, thus becoming a very useful aid to the development of the next generation of installations with substantially higher  $\beta$ s than now (5–10%), such as reactor designers would like them.

## REFERENCES

- Bateman, G. 1980 *MHD instabilities*, p. 977. The MIT Press.
- Connor, J. W., Hastie, R. J. & Taylor, J. B. 1979 *Proc. R. Soc. Lond A* **365**, 1–17.
- Degtyarev, L. M., Drozdov, V. V., Martynov, A. A. & Medvedev, S. Yu. 1984 In *Proc. 9th Int. Conf. on Plasma Physics, Lausanne, 27 June–3 July 1984* (ed. M. Q. Tran & M. L. Sawley), vol. 1, pp. 157–175.
- von Gierke, G. *et al.* 1985 Controlled fusion and plasma physics. In *Proc. 12th European Conference on Controlled Fusion and Plasma Physics, Budapest, 2–6 September 1985*. (*Europhysics conference abstracts* **9F** (1), 331–334.)
- Goedbloed, J. P. *et al.* 1985 Controlled fusion and plasma physics. In *Proc. 12th European Conference on Controlled Fusion and Plasma Physics, Budapest, 2–6 September 1985*. (*Europhysics conference abstracts* **9F** (1) 54–57.)
- Grimm, R. C., Greene, J. M. & Johnson, J. L. 1976 *Meth. computat. Phys.* **16**, 253.
- Gruber, R. *et al.* 1981 *Computer Phys. Commun.* **21**, 323.
- Overskei, D. O. & Strait E. J. 1986 MHD stability of tokamak experiments with high beta. In *Proc. Course and Workshop on Basic Physical Processes of Toroidal Fusion Plasmas, Varenna, Italy, 26 August–3 September 1985*, vol. 2. Brussels: CEE EUR 104 18EN.
- Saurenmann, H. *et al.* 1985 Report no. LRP 263/85. Centre de Recherches on Physique des Plasmas, Lausanne, Switzerland.
- Sykes, A. *et al.* 1983 Controlled fusion and plasma physics. In *Proc. 11th European Conference on Controlled Fusion and Plasma Physics, Aachen, 5–9 September 1983*. (*Europhysics conference abstracts* **2**, 363–366.)
- Troyon, F. & Gruber, R. 1985 *Physics Lett. A* **110**, 29.
- Wesson, J. 1978 *Nucl. Fusion* **18**, 87.

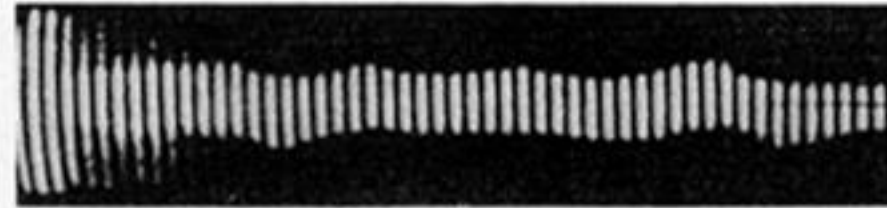


weaker  $B$  field      stronger  $B$  field



$m=0$       incompressible  
unstable deformation

FIGURE 1. Z-pinch ( $B_\theta, B_z = 0$ ). Side views of the evolution of an  $m = 0$  instability in a straight discharge with no axial field. The deformation exponentiates because of the increasing imbalance between the magnetic force and the plasma pressure.



$m=0$  stabilized

$m=1$  helicoidal

incompressible deformation,  
last to be stabilized

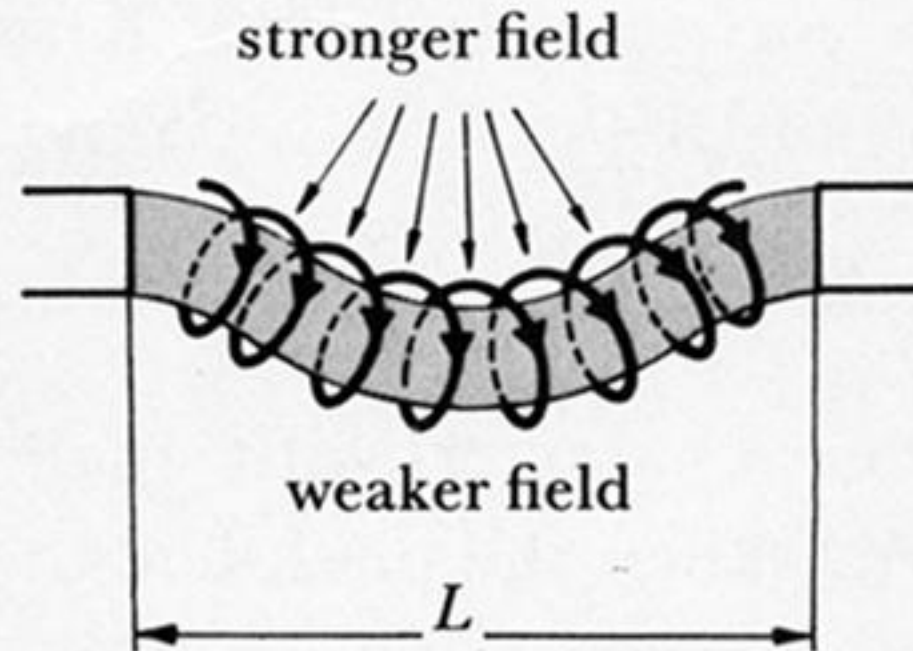


**FIGURE 2.** Stabilized Z-pinch ( $B_\theta$ ,  $B_z$  fields). Side views of the evolution of an  $m = 1$  kink instability in the same straight discharge in presence of a small axial field. The deformation is helicoidal and exponentiates at a rate a few times slower than the  $m = 0$  instability of figure 1. The force imbalance due to the higher magnetic force inside the kink drives it away from the straight equilibrium.

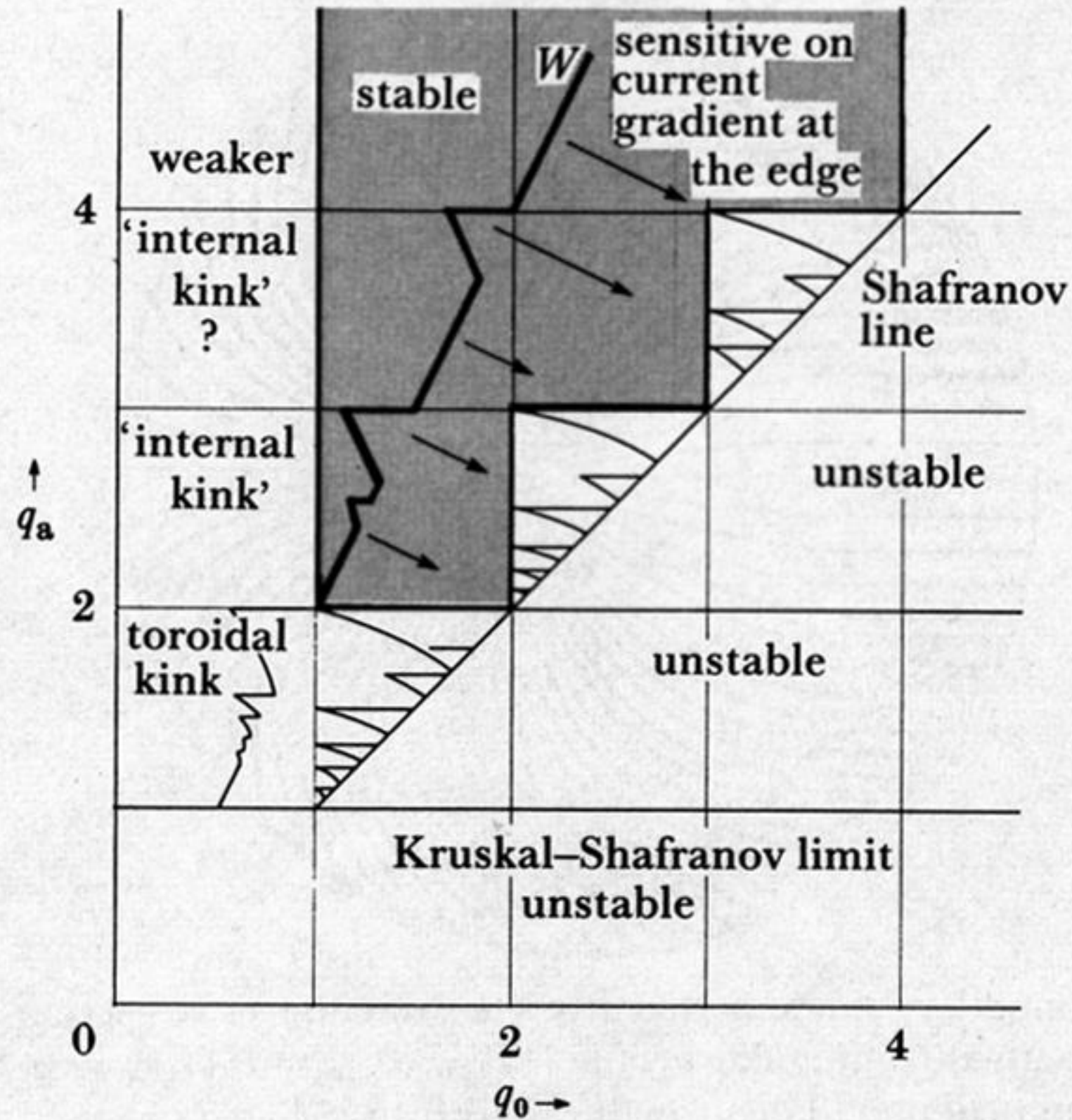


**FIGURE 3.** The stable operating range of a low  $\beta$ , large aspect ratio circular tokamak in the  $(q_0, q_a)$  plane. The right-hand boundary depends sensitively on the current profile.